Electronic Supplementary Material (ESI) for RSC Advances.

Supporting information

Interference micro/nanolenses of salts for local modulation of Raman scattering

Yun-Tae Kim,[†] Cheongha Lee,[†] Seongyeop Lim,[†] and Chang Young Lee[†,‡,*]

[†]School of Energy and Chemical Engineering, Ulsan National Institute of Science and Technology (UNIST), Ulsan 44919, Republic of Korea

[‡]Graduate School of Carbon Neutrality, Ulsan National Institute of Science and Technology (UNIST), Ulsan 44919, Republic of Korea

[*]Corresponding author: cylee@unist.ac.kr

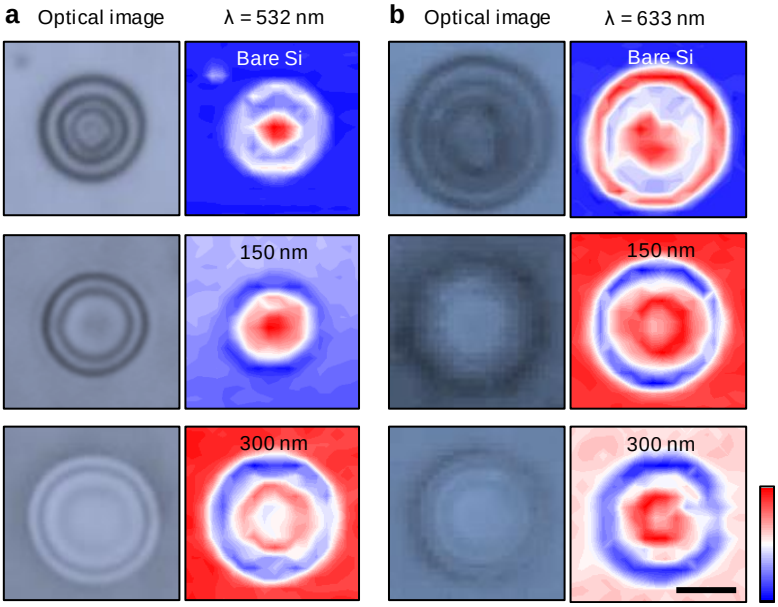

Figure S1. Focusing behaviors of microlenses under various interference conditions. Optical image (left) and corresponding Raman intensity maps (right) of silicon (520 cm^{-1}), modulated by a LiCl microlens placed on different oxide layers (bare, 150 nm, and 300 nm). The Raman maps were obtained using excitation wavelengths of 532 nm (a) and 633 nm (b). Scale bar: 3 μm.

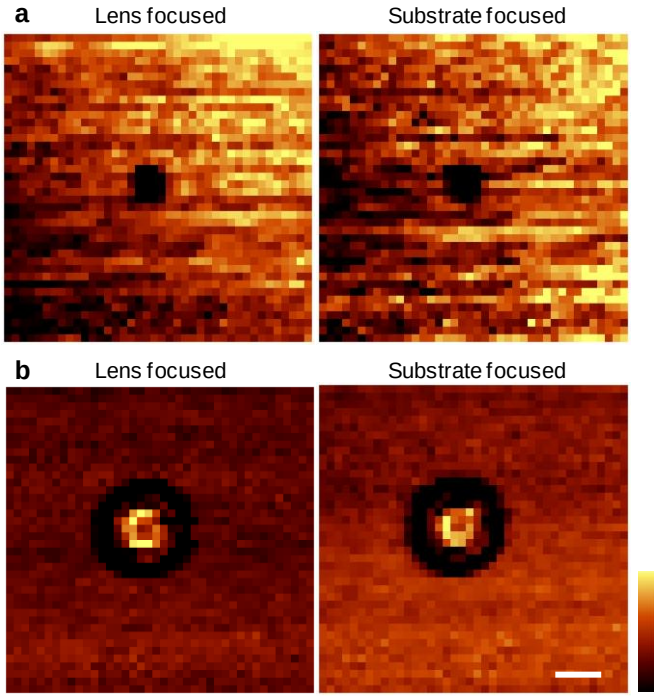

Figure S2. Independence of circular patterns through the lens on focusing points. Raman intensity maps of Si (520 cm^{-1}) in the focused through a LiCl lens (left) or on a substrate (right). (a) The small LiCl microlens (d ~1 μm) on 300-nm SiO_2/Si substrate upon excitation wavelength of 532 nm. (b) The LiCl microlens (d ~ 6 μm) on 300 nm SiO_2/Si substrate upon excitation wavelength of 633 nm. Scale bar: 3 μm.

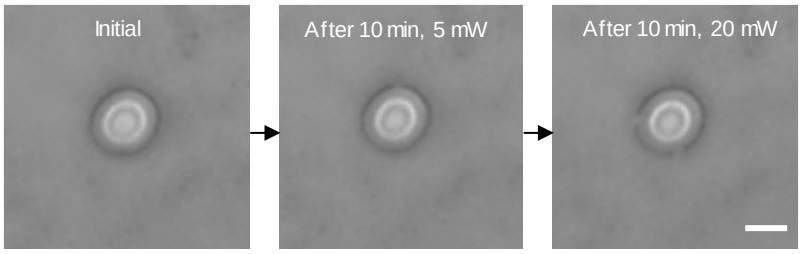

Figure S3. High stability of aqueous microlens under the laser irradiation. Optical images of 3 M LiCl microlens before (left), after first laser irradiation (5 mW, λ = 532 nm, for 10 min) (middle), and after second laser irradiation (20 mW, λ = 532 nm, for 10 min) (right) under the ambient condition (24.1 °C, 57% relative humidity). Scale bars: 3 μm.

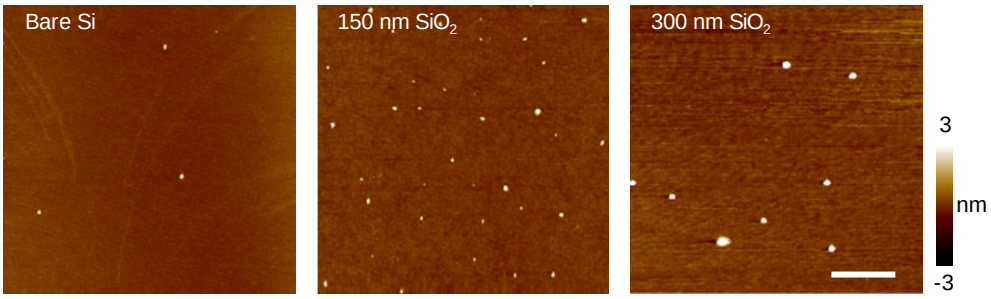

Figure S4. Surface roughness of silicon dioxide substrates with various oxide film thicknesses. Representative AFM images of bare Si (left), 150-nm SiO_2/Si substrate (middle), and 300-nm SiO_2/Si substrate (right). Scale bar: 1 μm.

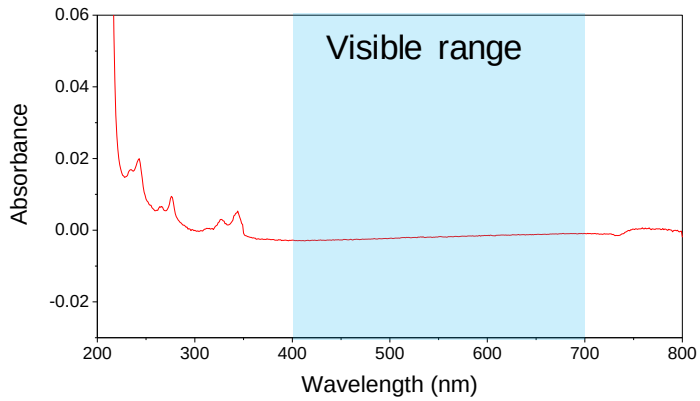

Figure S5. UV-Vis-NIR absorbance spectrum for saturated NaCl solution. Area shaded in blue indicates the visible range.

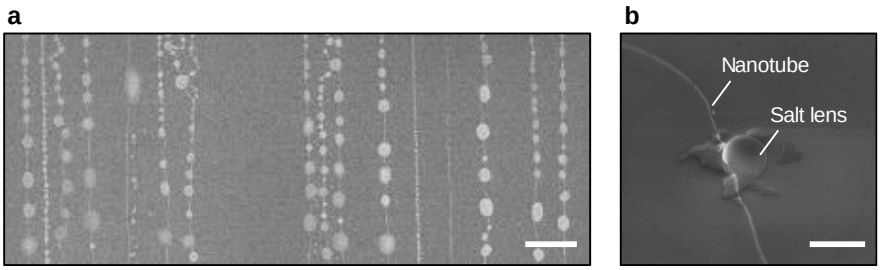

Figure S6. Decoration of salt micro/nanocrystals along carbon nanotubes via exterior transport. (a) SEM image after formation of salt lenses along the nanotubes via exterior transport of ions. Scale bar: 30 μm. (b) Tilted SEM image of a salt lens formed along nanotube. Scale bar: 500 nm

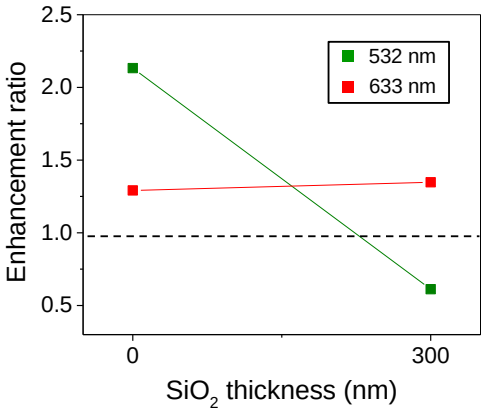

Figure S7. Modulation of Raman scattering of carbon nanotubes by interference lens. Enhancement ratio plotted versus thickness of oxide layer upon different excitation wavelengths.

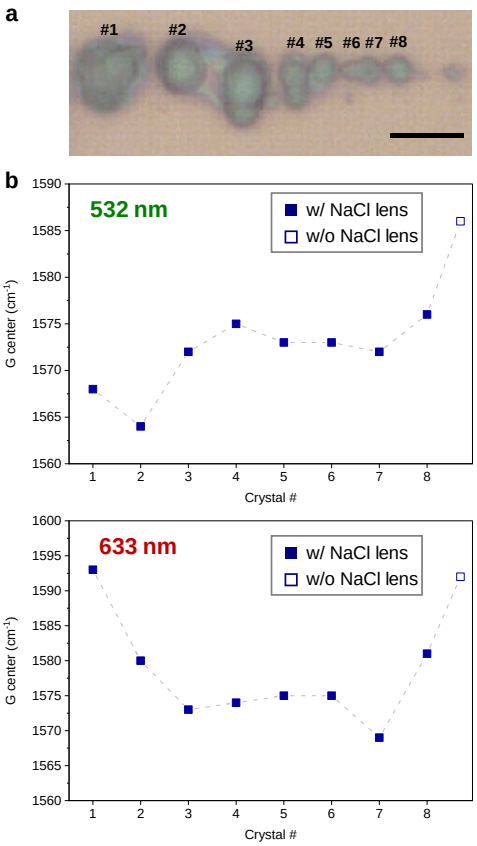

Figure S8. G-peak of SWNT down-shifted by salt microlenses. (a) Optical image of a SWNT decorated with NaCl lenses, labeled as #1 through #8, on a 300-nm SiO_2/Si substrate. Scale bars: 5 μm. **(b)** Peak center of G-peak obtained from each NaCl lens at 532 nm (top) and 633 nm (bottom) laser excitations.

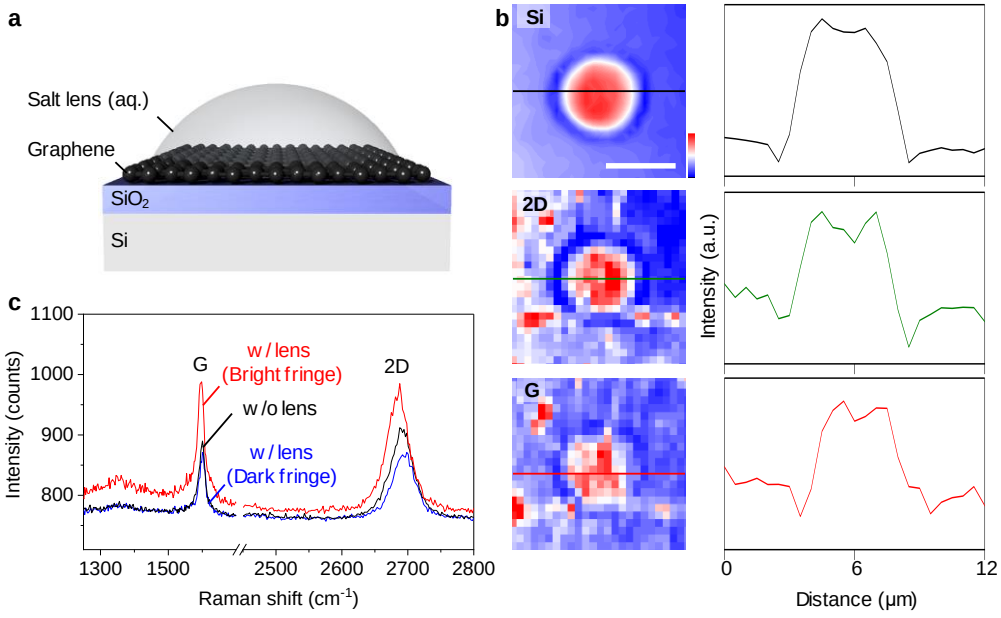

Figure S9. Circular fringe patterns of graphene in the Raman map. (a) Schematic illustrating a LiCl microlens placed on graphene/300-nm SiO_2/Si substrate. (b) Raman intensity maps and line profiles of silicon (520 cm^{-1}), 2D and G peak of graphene at 532 nm excitation, modulated by a LiCl microlens. Scale bar: 5 μm. (c) Representative Raman spectra of graphene collected without lens (black), from bright fringe within the lens (red), and from dark fringe within the lens (blue).